

**This is an electronic reprint of the original article.  
This reprint *may differ* from the original in pagination and typographic detail.**

**Author(s):** Gorelick, Sergey; Ylimäki, Tommi; Sajavaara, Timo; Laitinen, Mikko; Whitlow, Harry

**Title:** Development of a MeV ion beam lithography system in Jyväskylä

**Year:** 2007

**Version:**

**Please cite the original version:**

Gorelick, S., Ylimäki, T., Sajavaara, T., Laitinen, M., & Whitlow, H. (2007).  
Development of a MeV ion beam lithography system in Jyväskylä. Nuclear  
Instruments and Methods in Physics Research Section B: Beam Interactions with  
Materials and Atoms, 260(1), 77-80. <https://doi.org/10.1016/j.nimb.2007.01.260>

All material supplied via JYX is protected by copyright and other intellectual property rights, and duplication or sale of all or part of any of the repository collections is not permitted, except that material may be duplicated by you for your research use or educational purposes in electronic or print form. You must obtain permission for any other use. Electronic or print copies may not be offered, whether for sale or otherwise to anyone who is not an authorised user.

# 1 Development of a MeV ion beam lithography 2 system in Jyväskylä

3 Sergey Gorelick<sup>a,\*</sup>, Tommi Ylimäki<sup>a</sup>, Timo Sajavaara<sup>a</sup>,  
4 Mikko Laitinen<sup>a</sup>, Ananda Sagari A.R.<sup>a</sup>, Harry J. Whitlow<sup>a</sup>

5 <sup>a</sup>*Department of Physics, P.O.Box 35, FIN-40014 University of Jyväskylä, Finland*

---

## 6 Abstract

7 A lithographic facility for writing patterns with cyclotron beams is under develop-  
8 ment for the Jyväskylä cyclotron. Instead of focusing and deflecting the beam with  
9 electrostatic and magnetic fields a different approach is used. Here a small rectangu-  
10 lar beam spot is defined by the shadow of a computer-controlled variable aperture  
11 in close proximity to the sample. This allows parallel exposure of rectangular pat-  
12 tern elements of 5–500  $\mu\text{m}$  side with protons up to 6 MeV and heavy ions (<sup>20</sup>Ne,  
13 <sup>85</sup>Kr) up to few 100 MeV. Here we present a short overview of the system under  
14 construction and development of the aperture design, which is a critical aspect for  
15 all ion beam lithography systems.

16 *Key words:* MeV ion beam lithography, cyclotron, proximity aperture, proton  
17 beam writing

18 *PACS:* 01.52.+r, 06.60.Ei, 29.20.Hm, 81.40.Wx, 85.40.Hp, 87.80.-y

---

## 19 1 Introduction

20 MeV ion beam lithography is emerging as an advanced lithography tool for  
21 applications [1–7], which require extremely high line width to resist thickness  
22 aspect ratios [8,9]. Use of focused MeV proton beams from high-brightness

---

\* *Corresponding author:* S. Gorelick, Department of Physics, PO Box 35 (YFL),  
FIN-40014 University of Jyväskylä, Finland. tel: +358-14-260 2399, fax: +358-14-  
260 2351, e-mail: Sergey.Gorelick@phys.jyu.fi

1 electrostatic accelerators allows high spatial-density patterns to be written  
2 with line-widths on a few tens of nm scale. Cyclotron beams generally have  
3 higher energies, which enables pattern writing in thicker resists (up to 400  $\mu\text{m}$   
4 for 6 MeV protons in PMMA) [10]). However, even if large beam currents  
5 are available (up to 100's of  $\mu\text{A}$ ), the divergence is often large (about 1 mrad)  
6 which implies it is not straightforward, to use a magnetic focusing or proximity  
7 aperture approaches.

8 For our biomedical research programmes at a cellular and sub-cellular level  
9 [11] we are interested in rapidly exposing patterns with a large number of  
10 pattern elements of 10–300  $\mu\text{m}$  size over a large area in thick ( $\leq 200 \mu\text{m}$ ) resists  
11 and polymer films. For this purpose we are constructing an ion beam writing  
12 facility that is based on a computer-controlled aperture in close proximity to  
13 the sample. This allows entire rectangular pattern elements to be exposed in  
14 one step using proton beam lithography or single heavy-ion tracks.

## 15 **2 Experimental set-up**

16 The system is shown schematically in Fig. 1. The size and shape of the beam  
17 spot is defined by a computer-controlled aperture system that can be posi-  
18 tioned in close proximity (0.3–20 mm) from the sample surface. The size and  
19 divergence ( $< 0.7$  mrad) of the beam impinging on the computer-controlled  
20 aperture is defined by a water-cooled 1 mm diameter Ta aperture located  
21 1.78 m upstream close to the exit of the switching magnet. Focusing is carried  
22 out using a magnetic quadrupole pair further upstream. A fluorescent screen  
23 and Faraday cup as well as Si p-i-n diodes [12] are used for beam diagnostics  
24 and current measurement.

1 The principle of the aperture system is shown in Fig. 1. The sample is mounted  
2 on exchangeable sample holders that fit onto a computer-controlled  $x$ - $y$ - $z$  stage  
3 [13] that has 100 nm precision and approximately  $1\ \mu\text{m}$  accuracy (Fig. 1(b) and  
4 (c)). Two L-shaped aperture blades in close proximity to the sample surface  
5 cast a rectangular shadow on the sample that defines the shape of the beam  
6 spot on the surface. (Fig. 1(a)). Precise movement of each L-shaped blade in  
7 the  $X'$  and  $Y'$  directions using linear motion stages [13] defines the vertical and  
8 horizontal size of the aperture. One corner of the rectangular aperture remains  
9 in a fixed position, while the position of the other three corners depends on  $X'$   
10 and  $Y'$ . Then combination of the sample position  $(x, y, z)$  and the computer-  
11 controlled aperture  $(X', Y')$  allows rectangular pattern elements to be written  
12 over a  $20\times 20$  mm field. The maximum side length of the rectangular pattern  
13 elements can be up to  $500\ \mu\text{m}$  while the minimum side length is determined  
14 by the resist contrast and penumbra broadening. The apertures, sample stage  
15 and beam blanking are controlled with a LabView-control program.

16 The two L-shaped aperture blades are each made from two  $100\ \mu\text{m}$  thick  $8\times 15$   
17 mm Ta sheets. Each aperture blade must be sufficiently thick to completely  
18 stop the incident ions. Taking this thickness to be  $R_p + 2\sigma_p$ , where  $R_p$  and  
19  $\sigma_p$  is the projected range and projected range straggling, respectively, allows  
20 patterning with our system up to  $\sim 6$  MeV protons and a few hundred MeV  
21 heavy ions such as  $^{20}\text{Ne}$ ,  $^{85}\text{Kr}$  (see Fig. 2). Comparison of the aperture thick-  
22 ness for stopping the beam and the range in PMMA (a typical resist material)  
23 in Fig. 2) shows that up to  $400\ \mu\text{m}$  thick resist can be written with protons  
24 and  $\sim 150\ \mu\text{m}$  for heavy ions. This is well-matched to the capabilities of the  
25 Jyväskylä cyclotron which can deliver ions up to  $130\text{A}/q^2$  MeV. Ta was chosen  
26 as the aperture material because of the ease of working and its high  $Z$ , which

1 presents a high Coulomb barrier to most ions (11 MeV for protons, 21 MeV  
2 for  $^4\text{He}$ , 87 MeV for  $^{20}\text{Ne}$ , 262 MeV for  $^{85}\text{Kr}$  [14]). This is important in or-  
3 der to minimize spurious exposure of the resist by charged reaction products  
4 formed on the aperture edges, as well as undesirable neutron production as  
5 well as activation of the resist itself. Proton irradiation of polymers with ener-  
6 gies of 6 MeV, or lower, can result in production of short-lived  $^{13}\text{N}$  with a 9.96  
7 minutes half-life. The cross-section at 6 MeV for fusion reaction  $^{12}\text{C}(p,\gamma)^{13}\text{N}$   
8 well below the Coulomb barrier (11 MeV) was estimated to be  $6\ \mu\text{b}$  based on a  
9 quantum mechanical calculation using the parabolic potential approximation  
10 with a 5 MeV curvature parameter [15].

11 Experiment showed edge-polishing of the Ta blades clamped in a metal pol-  
12 ishing jig with 2000 grove SiC paper followed by diamond paste [16], resulted  
13 in an edge with better than 80 nm peak to valley deviation from straightness  
14 [17] over 3.6 mm, measured with a profiler(Fig. 3). Presumably, this can be  
15 further improved using finer diamond paste or sputtering.

16 The penumbra broadening is presented in Fig. 4(b) for different aperture -  
17 sample distances. Note that because of the aperture construction, the mini-  
18 mum separation, when the sample and last aperture blade are in contact, is  
19 3 times the aperture thickness ( $300\ \mu\text{m}$ ). Taking a realistic minimum gap of  
20  $600\ \mu\text{m}$  gives an edge penumbra broadening of 340 nm. This value represents  
21 an upper limit and the actual broadening is expected to be smaller because of  
22 concentration of the beam along paraxial directions. Thermal heating of the  
23 computer controlled aperture is an important issue because thermal expansion  
24 limits the rate of pattern writing. The fluence required to expose PMMA cor-  
25 responds to about  $10^{14}$  of 2 MeV  $\text{H}^+$  ions per  $\text{cm}^{-2}$  [18]. An exposure rate of  
26 one pattern element in 30 s requires  $0.6\ \mu\text{A}$  of protons into a  $1\ \text{cm}^2$  area onto

1 the first aperture and correspondingly a maximum heat load of 9.2 mW on  
2 the second aperture. For zero thermal resistance between the L-shaped blades  
3 and the mounting blocks, which are assumed to be cooled only by radiation,  
4 the corresponding linear change in aperture size is 14 nm for 10 mm between  
5 blade-tip and fixing point. The overall absolute accuracy of the patterns is  
6 then set by the combined accuracy of the ( $x$  and  $X'$ ) and ( $y$  and  $Y'$ ) linear  
7 motion slides and corresponds to 1.4  $\mu\text{m}$  over 20 mm with a precision of better  
8 than 140 nm. It should be noted that parallel exposure of an entire pattern  
9 element rather than exposing pixel by pixel dramatically reduces the problem  
10 of thermal drifts because the much faster writing speed, allows a significant  
11 reduction in beam current. At these exposure rates the beam is adequately  
12 blanked within 1.5–2  $\mu\text{s}$  by a TTL signal sent to the accelerator injection  
13 system [19].

14 Secondary and scattered particles from the aperture blade edges may to have  
15 degrade the pattern edge sharpness. No theoretical analysis was performed,  
16 however, pattern broadening due to the particles scattered by the aperture is  
17 believed on the basis of ref. [20] to be relatively small.

### 18 **3 Conclusions**

19 The new MeV ion beam lithography system being constructed at the Jyväskylä  
20 Cyclotron Laboratory is described. This system is based on a computer con-  
21 trolled aperture system that can simultaneously expose rectangular pattern  
22 elements up to 500  $\mu\text{m}$  side length over a  $20\times 20$  mm<sup>2</sup> field with low energy  
23 (6 MeV) protons for proton beam writing or up to a few hundred MeV heavy  
24 ions (Ne, Ar) for ion track patterning. The minimum exposed feature size set

1 by penumbra broadening is  $\sim 400$  nm for a  $600 \mu\text{m}$  proximity gap. The energy  
2 (2–1300 MeV) and ion range (from hydrogen to gold) available from Jyväskylä  
3 K130 cyclotron make the presented lithography setup a very versatile system.

#### 4 **Acknowledgements**

5 This work was carried out under the auspices of the Academy of Finland  
6 Centre of Excellence in nuclear and accelerator-based physics (Ref 213503).

#### 7 **References**

- 8 [1] F. Sun, D. Casse, J.A. van Kan, R.Ge, F. Watt, *Tiss. Eng.* 10 (2004) 267.
- 9 [2] K. Ansari, J.A. van Kan, A.A. Bettiol, F. Watt, *Appl. Phys. Lett.* 85 (2004) 476.
- 10 [3] A.A. Bettiol, T.C. Sum, J.A. van Kan, F. Watt, *Nucl. Instr. and Meth.* 210  
11 (2003) 250.
- 12 [4] T.C. Sum, A.A. Bettiol, S. Venugopal Rao, J.A. van Kan, A. Ramam, F. Watt,  
13 *Proc. SPIE* 5347 (2004) 160.
- 14 [5] J.A. van Kan, P.G. Shao, K. Ansari, A.A. Bettiol, T. Osipowicz, F. Watt, in  
15 *press*.
- 16 [6] H. Ottevaere, B. Volckaerts, J. Lamprecht, J. Schwider, A. Hermanne, I.  
17 Veretennicoff, H. Thienpont, *Jap. J. Appl. Phys.* 43 (2004) 5832.
- 18 [7] F. Munnik, F. Benninger, S. Mikhailov, A. Bertsch, P. Renaud, H. Lorenz, M.  
19 Gmur, *Microelectronic Engineering* 67-8 (2003) 96.
- 20 [8] H.J. Whitlow, M.L. Auželité, I.A. Maximov, J.A. van Kan, A. Bettiol and F.  
21 Watt. *Nanotechnology* 15 (2004) 223.

- 1 [9] J.A. van Kan, A.A. Bettiol and F. Watt, Appl. Phys. Lett. 83 (2003) 1629.
- 2 [10] J.F. Ziegler, SRIM-2003, from <http://www.SRIM.org>
- 3 [11] S. Gorelick, P. Rahkila, A. Sagari A.R., T. Sajavaara, S. Cheng, L.B. Karlsson,  
4 J.A. van Kan, and H.J. Whitlow, *Growth of bone-cells on lithographically modified*  
5 *surfaces*, submitted.
- 6 [12] Si PIN photodiode S1223-01, <http://www.hamamatsu.com>
- 7 [13] ESP300 1-3 Axis Motion Controller/Driver, MFA-CCV6 Miniature Linear  
8 Stages, <http://www.newport.com>
- 9 [14] Spectrometer calculator of J. Kantele, "Practical" Columb barrier.
- 10 [15] PACE4 code, part of LISE++ software, D. Bazin, O. Tarasov, M. Lewitowicz,  
11 O. Sorlin, Nucl. Instr. and Meth. A 482 (2002) 307.
- 12 [16] Diamond & tools PD0501/4HP, grain size 1/2-0  $\mu\text{m}$ .
- 13 [17] B46.1-2002 Surface roughness, waviness and lay, ISBN 0791828018.
- 14 [18] J.A. van Kan, J.L. Sanchez, B. Xu, T. Osipowicz, F. Watt, Nucl. Instr. and  
15 Meth. B 158 (1999) 179.
- 16 [19] E. Liukkonen, *New K130 Cyclotron at Jyväskylä*, in Proceedings on the 13th  
17 International Conference on Cyclotrons and their Applications, Vancouver 1992,  
18 pp. 22-27.
- 19 [20] M.L. Taylor, R.D. Franich, A. Alves, P. Reichart, D.N. Jamieson, P.N. Johnston,  
20 Nucl. Instr. and Meth. B (2006), in press.



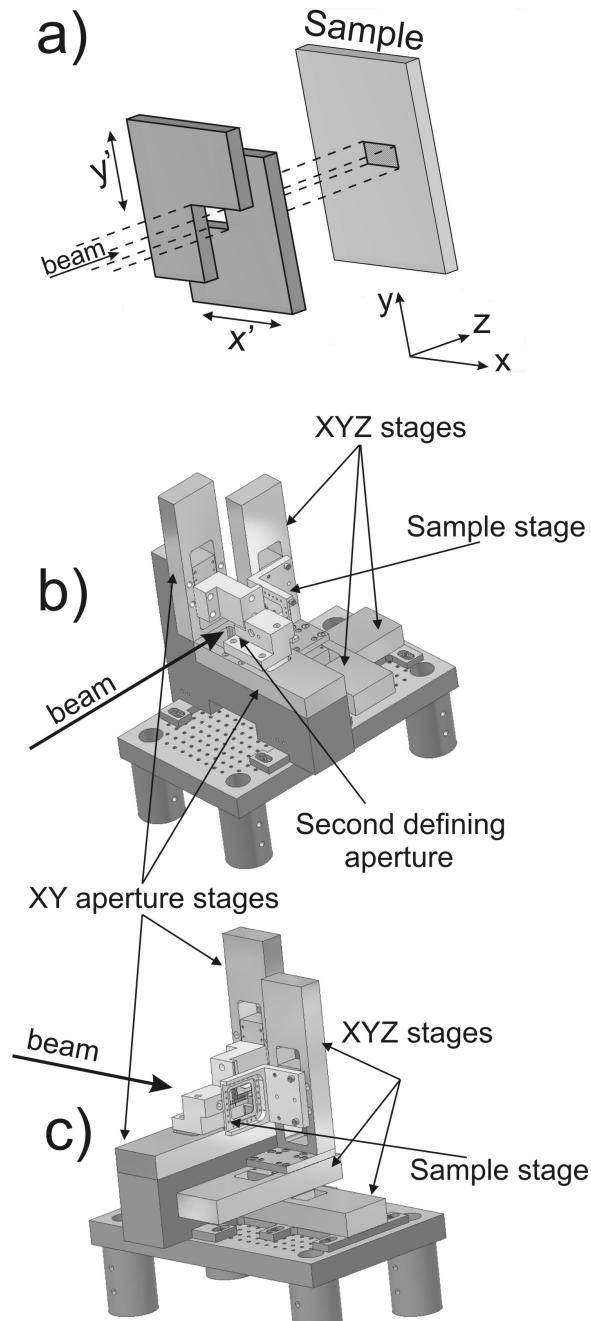


Fig. 1. Schematic layout of the ion beam lithography setup: The defining aperture. The opening of the aperture is controlled by relative motion of two tantalum L-shape plates. b) Aperture and sample are mounted on motorised stages. c) View from behind.

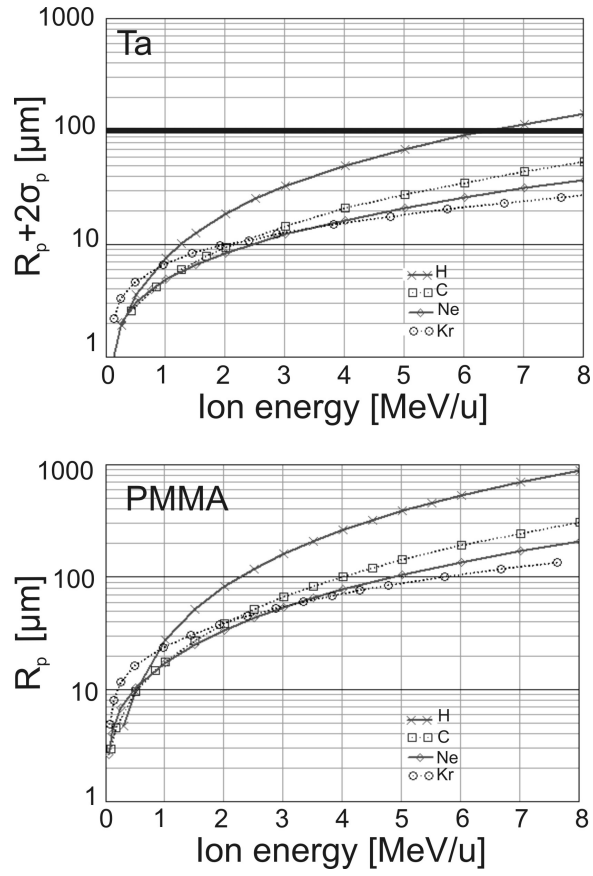


Fig. 2.  $R_p + 2\sigma_p$  of different ions in Ta vs. ion energy (top), range for different ions in PMMA vs. ion energy (bottom) [10].

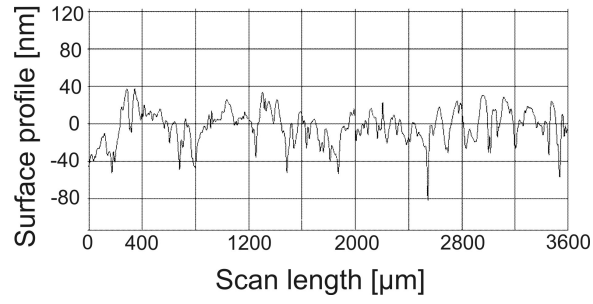


Fig. 3. Edge roughness of Ta aperture blade measured with a profiler after polishing with diamond paste.

1

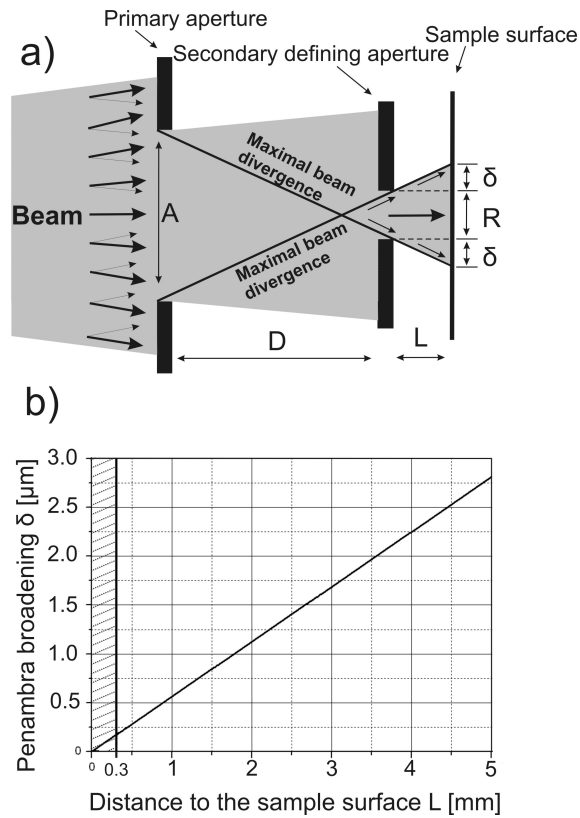


Fig. 4. a) Schematic of the collimation system. The primary aperture opening,  $A$ , is 1 mm in diameter, distance between the primary and the defining aperture,  $D$ , is 1.78 m,  $L$  is a distance between the sample surface the the defining aperture, and  $R$  is the opening of the defining aperture. b) Penumbra broadening,  $\delta$ , for different proximity of the defining aperture to the sample surface. The shaded area denotes the forbidden distances resulting from the finite aperture blade thickness.